



## How energy and water availability constrain vegetation water-use along the North Australian Tropical Transect

W. Zhuang<sup>a,b</sup>, L. Cheng<sup>c</sup>, R. Whitley<sup>d</sup>, H. Shi<sup>e</sup>, J. Beringer<sup>f</sup>, Y. Wang<sup>g</sup>, L. He<sup>h</sup>,  
J. Cleverly<sup>e</sup>, D. Eamus<sup>e</sup>, Q. Yu<sup>a,e,\*</sup>

<sup>a</sup>Key Laboratory of Water Cycle & Related Land Surface Processes, Institute of Geographic Sciences and Natural Resources Research, Chinese Academy of Science, Beijing 100101, China.

<sup>b</sup>University of Chinese Academy of Science, Beijing 100049, China.

<sup>c</sup>Water for a Healthy Country Flagship, CSIRO Land and Water, Canberra, ACT, Australia.

<sup>d</sup>Department of Biology, Macquarie University, NSW 2109, Australia.

<sup>e</sup>School of Life Sciences, University of Technology Sydney, P.O. Box 123, Broadway, NSW, 2007, Australia.

<sup>f</sup>School of Earth and Environment, The University of Western Australia, Crawley, WA, 6009, Australia.

<sup>g</sup>CSIRO Ocean and Atmosphere Flagship, Private Bag 1, Apsendale, Victoria 3195, Australia.

<sup>h</sup>National Meteorological Center, Beijing 100081, China.

\*Corresponding author. E-mail: yuq@igsnr.ac.cn

Received 25 March 2016; Accepted after revision 21 April 2016; Published online 24 May 2016

---

### Abstract

Energy and water availability were identified as the first order controls of evapotranspiration (ET) in ecohydrology. With a ~1,000 km precipitation gradient and distinct wet-dry climate, the North Australian Tropical Transect (NATT) was well suited for evaluating how energy and water availabilities constrain water use by vegetation, but has not been done yet. In this study, we addressed this question using Budyko framework that quantifies the evapotranspiration as a function of energy-limited rate and precipitation. Path analysis was adopted to evaluate the dependencies of water and carbon fluxes on ecohydrological variables. Results showed that the major drivers of water and carbon fluxes varied between wet and dry savannas: down-welling solar radiation was the primary driver of the wet season ET in mesic savanna ecosystems, while soil water availability was the primary driver in inland dryland ecosystems. Vegetation can significantly regulate water and carbon fluxes of savanna ecosystems, as supported by the strong link of LAI with ET and GPP from path analysis. Vegetation structure (i.e. the tree:grass ratio) at each site can regulate the impact of climatic constraint on ET and GPP. Sites with a low tree:grass ratio had ET and GPP that exceeded sites with high a tree:grass ratio when the grassy understory was active. Identifying the relative importance of these climate drivers and vegetation structure on seasonal patterns of water use by these ecosystems will help us decide our priorities when improving the estimates of ET and GPP.

**Keywords:** Evapotranspiration; Savannas; Energy limitation; Water limitation; GPP.

---

### Introduction

Evapotranspiration (ET) uses approximately 50% of the total solar radiation absorbed by the land surface, returning approximately 60% of the land surface rainfall annually to the atmosphere (Trenberth et al., 2009; Seneviratne et al., 2010). Vegetation productivity is tightly coupled with transpiration, which is a major component of ET. The first-order controls on ET are solar radiation and precipitation, as stated in the

Budyko model that is widely used in ecohydrological studies (Budyko, 1958; Zhang et al., 2001; Zhang et al., 2004; Donohue et al., 2007). Distinctly energy- and water-limited systems have been identified through ground observations and remote sensing data in Europe (Teuling et al., 2009), North America (Jones et al., 2012), China (McVicar et al., 2012), Brazil (da Rocha et al., 2009), Australia (Whitley et al., 2011), as well as at a global scale (Churkina and Running, 1998; Nemani et al., 2003).

Significant fractions of the estimated inter-annual variations in global ET and GPP have been attributed to semi-arid vegetation in the Southern Hemisphere, particularly in Australian ecosystems (Jung et al., 2010; Poulter et al., 2014). The tropical north of Australia is seasonally water-limited and the landscape is characterised by savanna ecosystems that are subject to distinct wet and dry seasons and annual rainfall driven by monsoonal weather systems (Nov–Apr; Bowman et al., 2010). The strength of the coupling between the land surface and the monsoon depression diminishes from the coast to the inland centre, creating a gradient in precipitation amount and variability. The North Australian Tropical Transect (NATT) was established to study the function of savanna ecosystems, the predominant landscape in north Australia (Koch et al., 1995; Hutley et al., 2001; Beringer et al., 2011a). Ecological functioning of savannas in drylands (i.e. hyper-arid, arid, semi-arid and dry sub-humid environments) is defined by seasonal variations in rainfall (i.e. having distinct wet and dry seasons) and resultant fluctuations in soil water availability (Eamus, 2003; Kanniah et al., 2010; Beringer et al., 2011b; Kanniah et al., 2011; Cleverly et al., 2013), while mesic savannas are limited by canopy light interception (i.e. available energy) (Whitley et al., 2011). Globally, other savanna sites have shown similar gradients in rainfall and energy *versus* water limitations. For example, along a biome gradient in Brazil (tropical forest to savanna), the factor controlling seasonality in evapotranspiration shifted from atmospheric evaporative demand in the wetter forests to soil moisture supply in the drier savanna (da Rocha et al., 2009). However, the degree of energy or water limitations has not been quantified previously across the NATT.

In general, the vegetation of the NATT is characterized by a coexistence of overstorey tree and understorey grass. Perennial C<sub>4</sub> grasses die back during the long dry season, which contributes considerably to the seasonal variations in tree:grass ratio. The tree:grass ratio is also affected by disturbances from nature and human activities (e.g. fire, cyclone, conversion of savanna to pasture). The contribution of the tree:grass ratio to ET and GPP along the NATT has been studied previously by Hutley et al. (2000) and Whitley et al. (2011). More than 75% of the total wet season ET is from the understorey (grass transpiration plus soil evaporation) (Hutley et al., 2000) and C<sub>4</sub> grasses contribute approximately 40% of annual total GPP at a mesic site (Howard Springs; Whitley et al., 2011). Considering the large proportion of ET and GPP from understorey grasses, the tree:grass ratio is an important variable for estimating the regional water balance and carbon sinks/sources.

Measurements using eddy flux technique has been widely used to evaluate the dependencies of water and carbon fluxes on environmental factors (Baldocchi et al., 2001; Hutley et al., 2005). Here we use eddy flux observation along the NATT to analysis and present ET and GPP in parallel. Our study aims to: 1) identify the threshold between energy and water limitations on ET and GPP along the north-south precipitation gradient; 2) determine how the tree:grass ratio affects ET and GPP.

## Materials and Methods

### Study Area

The flux sites used in this study represent different ecosystems spanning a distance of approximately 1000 km from the northern coastline to the central inland of the Australian continent along the NATT. Over this distance, annual rainfall decreases from over 1700 mm (mesic regions) to ~300 mm (xeric regions) (Figure 1). Along the NATT, vegetation shifts from tropical savanna to semi-arid grassland and woody savanna (Williams et al., 1996; Beringer et al., 2011a; Hutley et al., 2011; Eamus et al., 2013). Mesic sites that are influenced by the monsoon depression experience a stable onset and timing in seasonal transition periods, with the wet season typically lasting from November to April and the dry season from May to October. The duration of the dry season increases and the start of the wet season delays with increasing latitude (Cook and Heerdegen, 2001; Ma et al., 2013). The months April, November and December are transition periods between wet and dry seasons. Thus, we use the period January–March to represent wet season and the period May–October to represent dry season for all sites in this study.

We selected six flux sites of NATT located from north to south: Howard Springs (AU-How), Daly River Pasture (AU-DaP), Daly River Savanna (AU-DaS), Dry River (AU-Dry), Sturt Plains (AU-Stp) and Alice Springs (AU-Asm). These sites have been previously described by Beringer et al. (2007), Hutley et al. (2011) and Eamus et al. (2013). AU-How has the longest span of observation, from 01/2001 to 06/2015 (ongoing). The geographical locations, mean annual precipitation (MAP), dryness index ( $\Phi$ , defined in Section 2.3) and species composition for each site are given in Table 1. Dryland is defined by its  $\Phi > 1.5$  and thus AU-How, AU-DaP, AU-DaS are mesic ( $\Phi < 1.5$ ), AU-Dry and AU-Stp are dry sub-humid ( $\Phi: 1.5-2$ ) and AU-ASM is the only semi-arid site ( $\Phi: 2-5$ ) (Safriel et al., 2005). Four of these sites represent typical Australian savanna, characterised by a coexistence of evergreen trees with an understory of  $C_4$  grasses, while the remaining two sites AU-DaP and AU-Stp are a pasture land and a Mitchell grassland, respectively. Additionally, these flux sites are dominated by red kandosol soils, with the exception of AU-Stp, which is underlain by a black cracking clay in a grey vertisol soil profile.

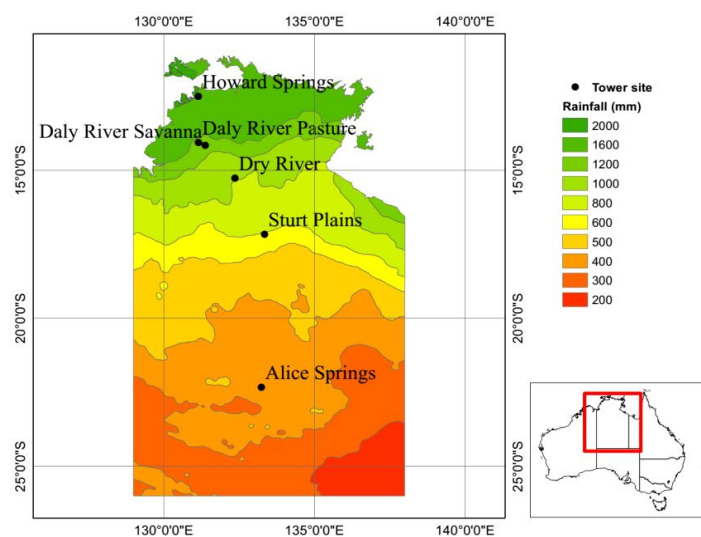


Figure 1. Geographic location and precipitation distribution of the study area Northern Australian Tropical Transect (NATT). The six flux tower sites investigated are labelled on the map.

Table 1. Key features of the selected six eddy flux sites used in this study after Hutley et al. (2011) and Glenn et al. (2011). MAP was calculated during the year 2000-2007.

Site	Climate Regimes	MAP (mm)	Dryness Index	Location	Vegetation type	Data period
AU-How	mesic	1714	0.99	12° 29' 39.12" S, 131° 09' 09" E	Open-forest savanna	01/2001-06/2013
AU-DaP	mesic	1250	1.29	14° 03' 48" S, 131° 19' 05" E	Improved tropical pasture	01/2007-09/2013
AU-DaS	mesic	1170	1.26	14° 09' 33.12" S, 131° 23' 17.16" E	Woodland savanna	01/2007-07/2013
AU-Dry	dry sub-humid	850	1.82	15° 15' 31.62" S, 132° 22' 14.04" E	Woodland savanna	01/2008-06/2013
AU-Stp	dry sub-humid	535	1.90	17° 09' 2.76" S, 133° 21' 1.14" E	Mitchell grassland	01/2008-06/2013
AU-Asm	semi-arid	305.9	5.00	22.3° S, 133.2° E	Acacia savanna woodland	09/2010-09/2013

### *Eddy Flux Data and LAI*

The flux data were available from the Australia and New Zealand Flux (OzFlux) Research and Monitoring Network (<http://www.ozflux.org.au/>) and the Australian Supersite Network (e.g. Cleverly, 2011). The data were level 4 (meteorological gaps filled, flux gaps unfilled), or half-hourly data. The variables used in our study include air temperature ( $T_a$ ), precipitation (ppt), vapour pressure deficit (VPD), wind speed, upwelling shortwave radiation ( $S_d$ ), net radiation ( $R_n$ ), ground heat flux ( $G$ ), net ecosystem exchange (NEE), soil water content (SWC), ET, etc. SWC were measured at the depth of 10 cm and 5 cm for the site AU-Asm and the remaining five sites, respectively. Gross Primary Productivity (GPP) was not observed but was estimated as the sum of NEE and ecosystem respiration ( $R_e$ ).  $R_e$  was assumed to be equal to night time NEE under sufficient wind speed (the wind fraction  $> 0.15 \text{ m s}^{-1}$ ). The advanced processing and quality control were used to fill gaps in meteorology, soil moisture and fluxes using the Dynamic INtegrated Gap filling and partitioning for Ozflux (DINGO) system (Beringer et al., 2007; Haverd et al., 2012; Shi et al., 2014). Leaf area index (LAI) was derived from MODIS (Moderate Resolution Imagine Spectroradiometer sensor) 8 day 500 m product. The size of MODIS image approximately amount to that of the tower footprint. LAI time series were extracted with a central 3\*3 km window (Rahman et al., 2005; Xiao et al., 2005) and smoothed with the TIMESAT tool (Jönsson and Eklundh, 2004).

### *The Budyko Framework*

In the Budyko framework, ET is limited by the availability of either water or energy. If water supply is sufficient and all available energy is converted to  $\lambda E$ , ET amounts to  $R_n/\lambda$ , where  $\lambda$  ( $2.45 \times 10^6 \text{ J kg}^{-1}$  at 20 °C) is the latent heat of vaporisation. Budyko (1974) considered  $R_n/\lambda$  as “the greatest possible value of evaporation under given conditions” defined by line AB in Figure 2. If energy supply is sufficient and all

the precipitation is returned to atmosphere through ET, ET equals precipitation, as illustrated by line BC in Figure 2. Normally, most observations were located below line AB and line BC, forming the Budyko curve (i.e. the function of evaporative index to dryness index). Here, the evaporative index ( $\varepsilon$ ) equals to the ratio of annual ET to ppt and the dryness index equals the ratio of annual  $R_n/\lambda$  to ppt. Values of  $\Phi > 1$  indicate a water-limited environment and  $\Phi < 1$  represents energy-limitation. The difference between  $\varepsilon$  and the water limitation line (where  $\varepsilon = 1$ ) is generally taken to represent water lost as run-off (Raupach, 2001; Donohue et al., 2007). Here we use Budyko framework at site scale to evaluate water and energy limitations on ET along NATT.

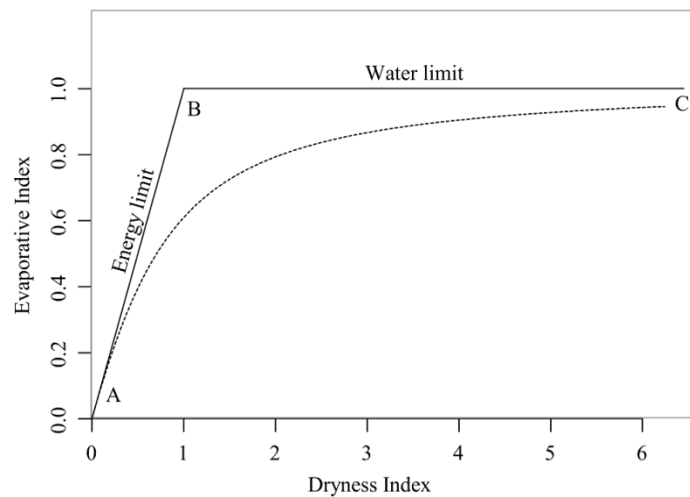


Figure 2. Budyko framework and curve after Donohue et al. (2007). The dotted curve describes the relationship between dryness index and evaporative index. Line AB defines the energy limit to ET and line BC defines the water limit.

Whenever the observed rainfall at the flux site was not available, we used rainfall observation at the BoM (the Bureau of Meteorology of Australia) station (available at [www.bom.gov.au](http://www.bom.gov.au)) nearest to each site. Annual  $R_n$  and ET were calculated from tower based data. We also used the analytical equation developed by Fu (1981) to depict Budyko curve (Zhang et al., 2004):

$$\varepsilon = 1 + \Phi - [1 + \Phi^w]^{1/w} \tag{Eq. 1}$$

where  $w$  is a parameter determining the shape of Budyko curve.

To capture seasonal variations of the limitation regimes of ET, we use the Priestley-Taylor coefficient ( $\alpha$ ) (Priestley and Taylor, 1972) that is estimated as the ratio of evapotranspiration to equilibrium evaporation ( $\lambda E_{eq}$ ):

$$\alpha = \lambda E / \lambda E_{eq} \tag{Eq. 2}$$

When  $\alpha > 1.0$ , sufficient water is available and ET is controlled by available energy. Equilibrium evaporation is mainly limited by available energy and is the lower limit of wet surface evaporation if advection is ignored (Raupach, 2001):

$$\lambda E_{eq} = \frac{\Delta}{\Delta + \gamma} (R_n - G) \quad (\text{Eq.3})$$

### Data Analysis

We used linear regression and path analysis to examine the dependencies of water and carbon fluxes on  $S_d$  and SWC at these selected sites. Daily averages during rain-free periods that did not violate conditions of statistical stationarity in the measured turbulent fluxes were used for path analysis and linear regression. Although similar to multiple regression, path analysis can estimate the strength and relative importance of the assumed casual relationships among variables (Li, 1981). Path analysis is most effective in the absence of feedbacks and for evaluating data in which independence among variables is not certain, rendering more common multiple regression techniques inappropriate (Huxman et al., 2003). It has often been used in the analysis of crop yield (Dewey and Lu, 1959). Recently, path analysis has been applied to leaf/canopy scale gas exchange data to evaluate the relative influences of various micrometeorological factors on ecosystem water and carbon fluxes in a North American deciduous forest (Bassow and Bazzaz, 1998), a high-elevation subalpine forest (Huxman et al., 2003), a northeastern Tibetan Plateau alpine meadow (Saito et al., 2009), an Alaskan coastal plain tundra (Olivas et al., 2010), a black spruce forest in interior Alaska (Ueyama et al., 2014), various terrestrial ecosystems of China (Tang et al., 2014; Zhu et al., 2015) and a tropical savanna in Brazil (Rodrigues et al., 2014).

Here we applied path analysis to ET and GPP, respectively. In our conceptual model for path analysis, we assumed that  $S_d$ , LAI and SWC constrained ET directly and  $T_a$  constrained ET indirectly through VPD;  $S_d$ ,  $T_a$ , LAI and SWC played important roles in driving or constraining GPP directly and LAI was affected by SWC. Path analysis was conducted using the R package lavaan (Latent Variable Analysis, V0.5-16) (Rosseel, 2012). In path analysis, the path values are standardized and therefore the relative importance of ecohydrological variables on ET or GPP can be compared (Grace and Bollen, 2005).

## Results and Discussions

### Site-specific Budyko Curves

We fitted the Budyko curve to the annual evaporative index and dryness index from each site according to the Fu' equation (Eq. (1)) and values of the only parameter  $w$  were given (Figure 3). Overall,  $\varepsilon$  increased with  $\Phi$ . Most points lied below the lines of energy or water limit (Figure 3.a). Two points corresponding to  $\varepsilon > 1$  may be caused by a number of factors: e.g. biases in rainfall or ET, or lack of hydrological equilibrium at annual timescale (Donohue et al., 2010; Donohue et al., 2012). The values of parameter  $w$  were over 2.0 at savanna sites except for AU-Asm and less than 2.0 for pasture site AU-DaP, grassland site AU-Stp and the Mulga site AU-Asm. The average annual  $\Phi$  was lowest at AU-How (0.99) and highest at AU-Asm (5.00). AU-DaP and AU-DaS had similar  $\Phi$  (1.29 and 1.26, respectively). AU-How was most strongly limited by energy, while AU-Asm was most strongly limited by precipitation (Figure 3.b).

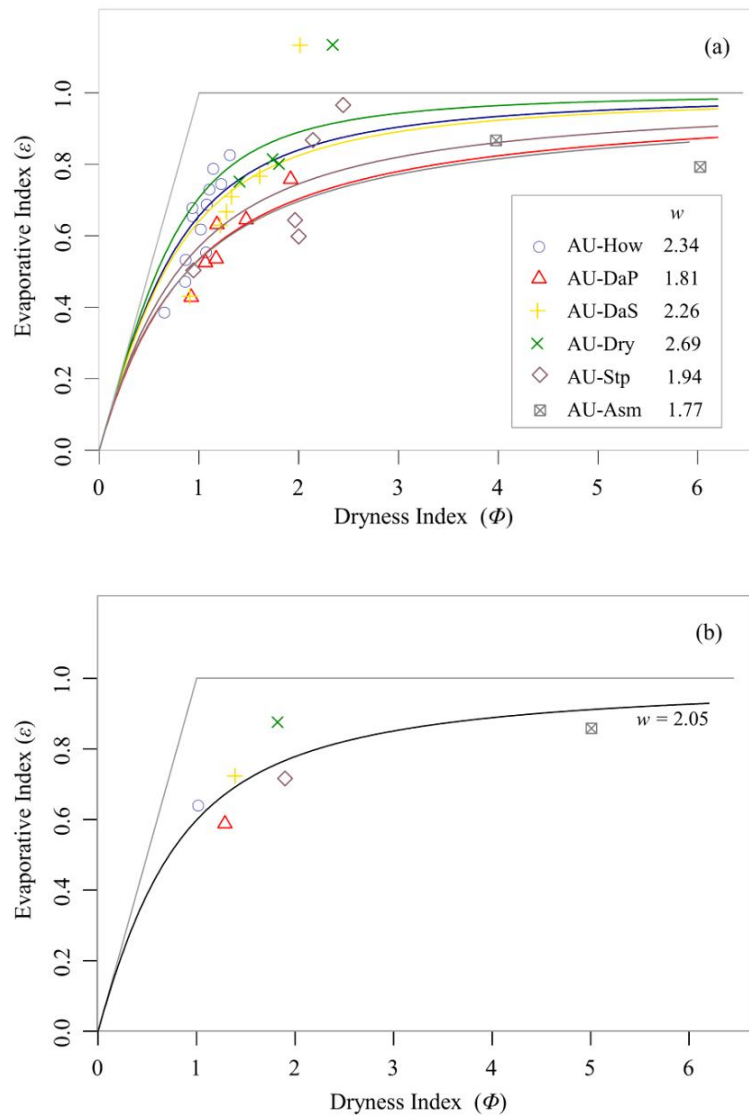


Figure 3. Budyko framework and curves of six selected sites along NATT. Each data point represents 1 year excluding incomplete year 2013 (Panel (a)) and mean annual value for each site (Panel (b)), respectively.

### Dependencies of ET and GPP on Energy and Water Availability

Climate conditions at AU-How during a typical hydrological year (2011-2012) was illustrated in Figure 4: 1) November-March was characterized by high precipitation, high temperature and humid air (average VPD less than 1 kPa); 2) June- July (named cool dry period) was characterized by relatively low  $T_a$  but high VPD; 3) during August-September, tropical savannas entered the hot dry period with high  $T_a$  and VPD (Braithwaite and Estbergs, 1988; Williams et al., 1997). During August-September, tropical savannas entered the hot dry period characterized by high  $T_a$ , increased  $S_d$ , high VPD and low SWC (Figure 4).

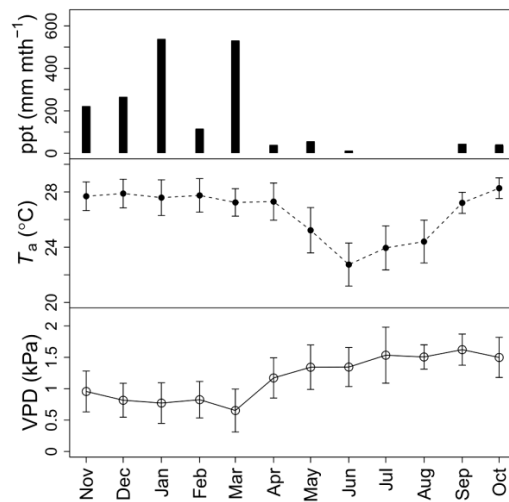


Figure 4. Monthly precipitation (black column), average air temperature (black point) and VPD (circle) at AU-How in the 2011-2012 hydrological year.

During the wet season and the cool dry period, ET of AU-How closely followed the changes of  $E_{eq}$ . Apparent differences between ET and  $E_{eq}$  were observed in the hot dry period at AU-How (Figure 5). At the AU-DaP site, ET was close to  $E_{eq}$  during the wet season, but declined at the onset of the dry seasons. At the AU-DaS site, ET and  $E_{eq}$  approached their respective peaks around February and then declined until the cool dry period, remaining low ( $\sim 1 \text{ mm day}^{-1}$ ) throughout this period. At the AU-Dry and AU-Stp sites, the difference between  $E_{eq}$  and ET during the wet season was largely apparent during prolonged rainless periods. At the driest site AU-Asm, ET followed the precipitation pulses rather than  $E_{eq}$ , although  $E_{eq}$  became as small as ET during individual rainfall events (Figure 5).

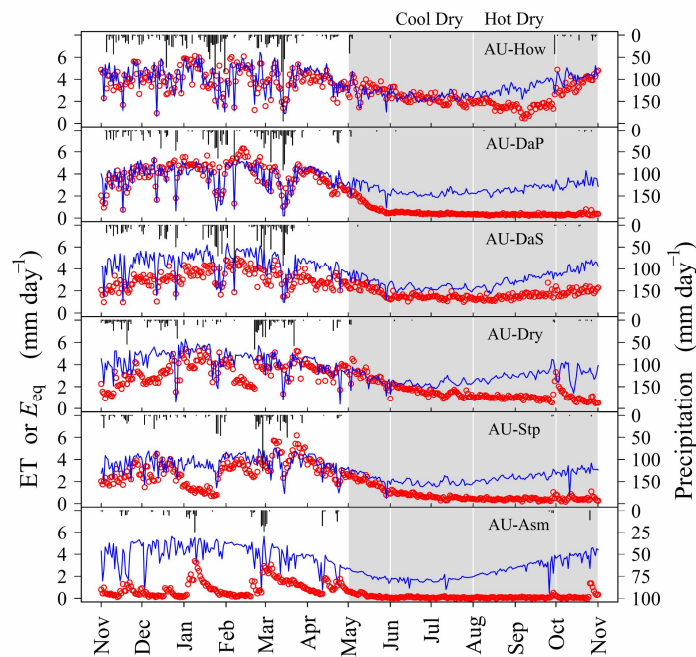


Figure 5. Time series of daily equilibrium ET ( $E_{eq}$ , blue lines), actual ET (red points) and precipitation at the six sites during the 2011-2012 hydrological year.

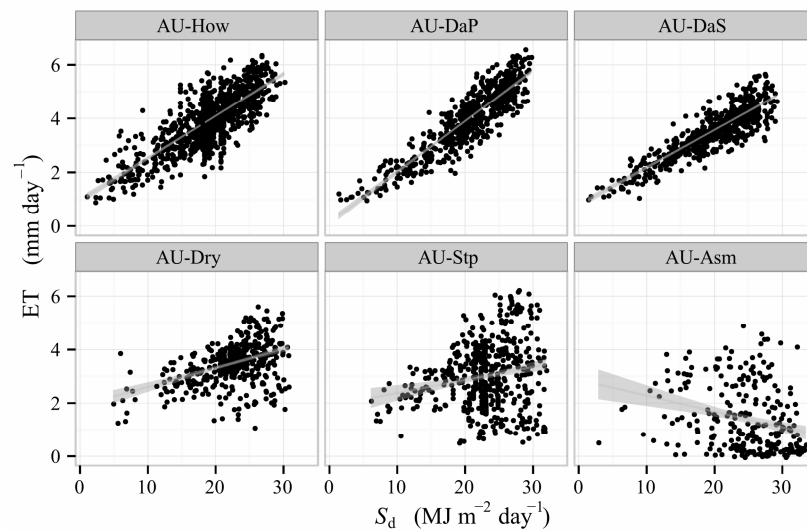


Figure 6. Wet season (Jan–Mar)  $S_d$  and ET at the six selected sites during the entire time series available indicated in Table 1.

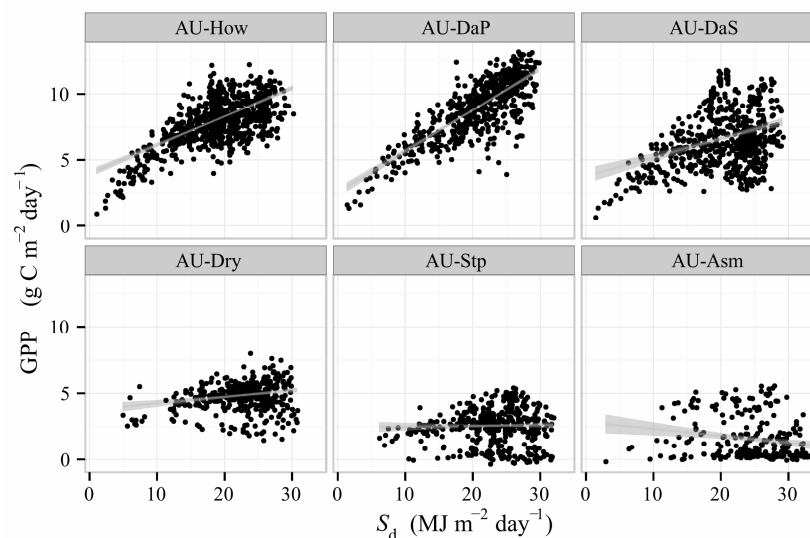


Figure 7. Wet season (Jan–Mar)  $S_d$  and GPP at the six selected sites during the entire time series available indicated in Table 1.

Regression analysis illustrated that  $S_d$  had a significantly positive relationship with ET in the wet and mesic sites AU-How, AU-DaP and AU-DaS during wet season (Jan–Mar) ( $R^2$  equals 0.606, 0.794, 0.760\*\*\*, respectively, Figure 6). The linear relationships between ET and  $S_d$  deteriorated at the drier end of the NATT (Figure 6). The relationships of  $GPP \sim S_d$  was similar to that of  $ET \sim S_d$  (Figure 7). GPP was significantly correlated with  $S_d$  at the mesic sites of AU-DaP ( $R^2 = 0.643$ \*\*\*), AU-How ( $R^2 = 0.399$ \*\*\*) and AU-DaS ( $R^2 = 0.127$ \*\*\*). Poor correlations of  $GPP \sim S_d$  were found at the dryland sites of AU-Dry ( $R^2 = 0.05$ \*\*\*), AU-Stp (nonsignificant,  $P = 0.001$ ) and AU-Asm (nonsignificant,  $P = 0.001$ ).

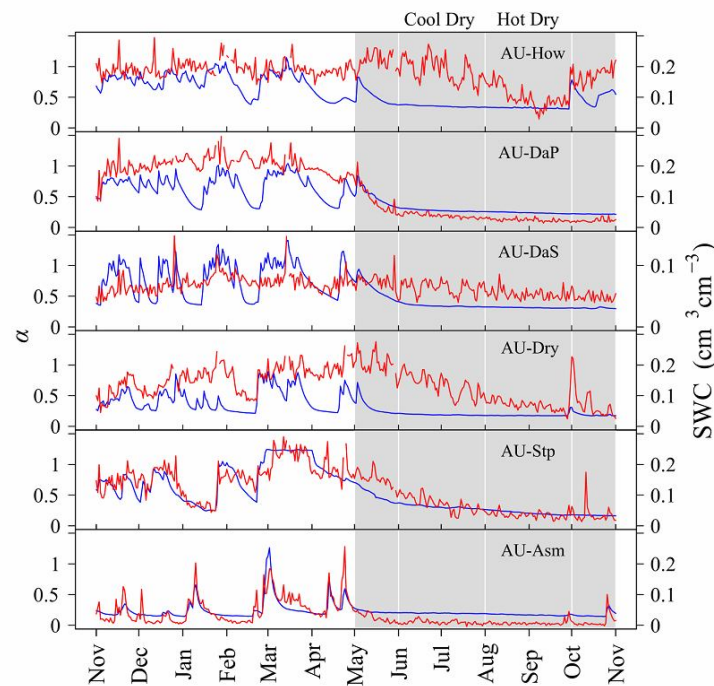


Figure 8. Time series of daily Priestley-Taylor coefficient ( $\alpha$ , red curves) and soil water content (SWC) at the depth of 5 cm (blue curves) at the six selected sites during the entire time series available indicated in Table 1.

The Priestley-Taylor coefficient  $\alpha$ , which represents normalized evaporation (Baldocchi et al., 2004), was used to dismiss the influences of net radiation on ET. The variations of  $\alpha$  with SWC during the 2011-2012 hydrological year were illustrated in Figure 8. At the AU-How site,  $\alpha$  was insensitive to declining soil water content except during the hot dry period of the late dry season before the return of the rains (Figure 8). At AU-DaP,  $\alpha$  was maintained around 1.0 during wet season and declined with the decreasing SWC in dry season.  $\alpha$  fluctuated above 0.5 at AU-DaS.  $\alpha$  approached the lowest values at the end of dry season at AU-Dry. For the three savanna sites AU-How, AU-DaS and AU-Dry,  $\alpha$  was insensitive to the rapid decline of SWC during the transit of wet and dry seasons (Figure 8) and this insensitivity contributed to their low  $R^2$  of  $\alpha \sim \text{SWC}$  (0.237, 0.279, 0.287, respectively, Figure 9). In contrast,  $\alpha$  was sensitive to the variations of SWC at AU-Stp and AU-Asm, resulting a significantly positive correlations for  $\alpha \sim \text{SWC}$  ( $R^2$  equals 0.700, 0.662,  $P < 0.005$ , Figure 9). GPP was most sensitive to SWC at the sites AU-DaP and AU-Stp ( $R^2$  equals 0.550, 0.505\*\*\*, respectively, Figure 10), followed by that of AU-How and AU-DaS ( $R^2$  equals 0.444, 0.313\*\*\*, respectively). However, the relationship of GPP  $\sim$  SWC was less significant at AU-Dry and AU-Asm ( $R^2$  equals 0.182, 0.193\*\*\*, respectively).

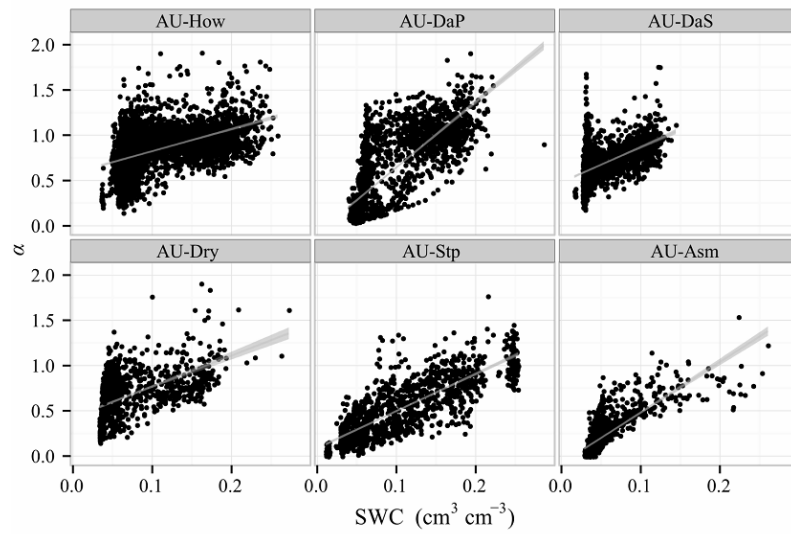


Figure 9. Wet season (Jan–Mar) SWC and  $\alpha$  at the six selected sites during the entire time series available indicated in Table 1.

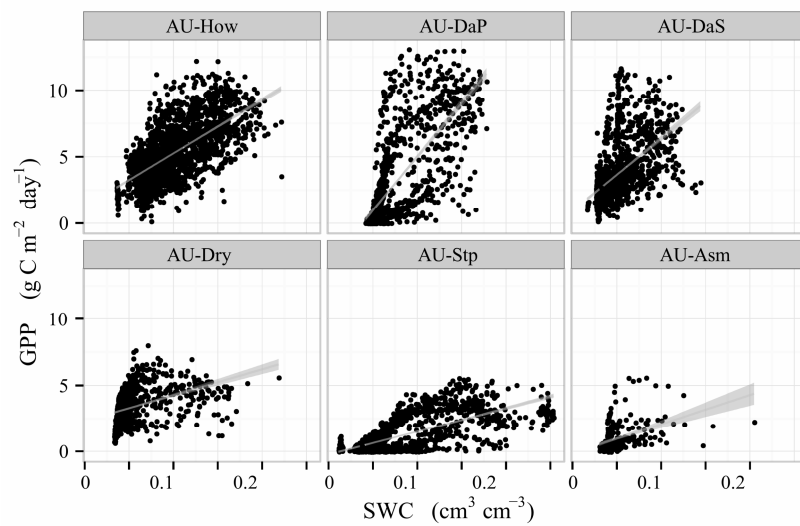


Figure 10. Wet season (Jan–Mar) SWC and GPP at the six selected sites during the entire time series available indicated in Table 1.

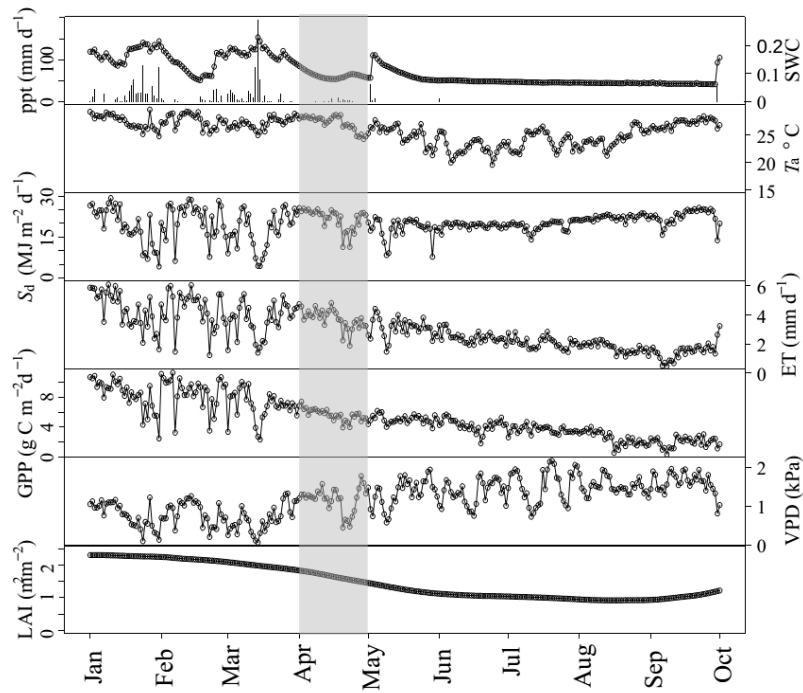


Figure 11. Time series of daily  $S_d$ ,  $T_a$ , VPD, SWC, LAI, ET and GPP at AU-How during 01/2012-09/2012.

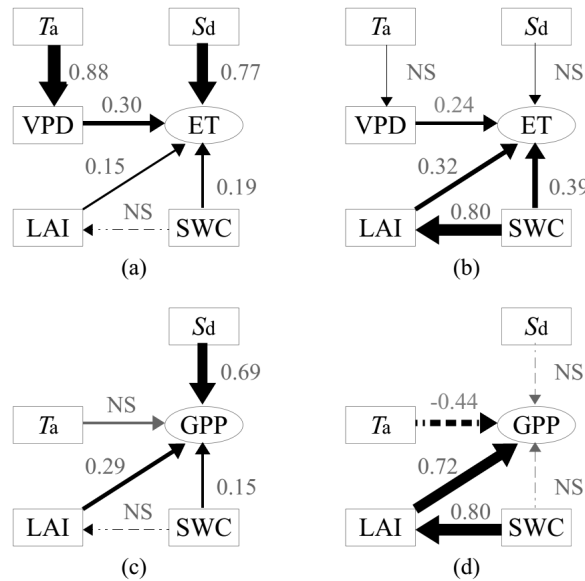


Figure 12. Diagram of path analysis illustrating the relative importance of the ecohydrological variables  $S_d$ ,  $T_a$ , VPD, SWC and LAI on ET during 01/2012-03/2012 (a) and during 05/2012-10/2012 (b) and path diagram illustrating the relative importance of  $S_d$ ,  $T_a$ , SWC and LAI on GPP during 01/2012-03/2012 (c) and during 05/2012-10/2012 (d). The thickness of each arrow and the value beside it represent the path coefficients. Solid arrows represent positive correlations and dashed ones are negative correlations. Paths that are not significant at  $P < 0.05$  are indicated as “NS”; all other paths are significant at the  $P < 0.05$  level. In the path diagram, the thickness of the arrow represents the path value (i.e. the relative strength of a specific relationship).

Path diagrams of two different period at AU-How are illustrated in Figure 12. During the period 01/2012-03/2012 (representative wet season),  $S_d$  was the primary direct factor controlling ET and GPP (Figure 12.a & 12.c), evident in the nearly synchronized variations of daily averages of  $S_d$ , ET and GPP (Figure 11). During the period 05/2012-09/2012 (representative dry season), SWC and LAI were the primary direct factors controlling ET (Figure 12.b), evident in the synchronized declining trend of ET, SWC and LAI; LAI was the primary factor controlling GPP (Figure 12.d). Figures 11 and 12 illustrate that path analysis is capable of identifying the primary factors controlling water and carbon flux.

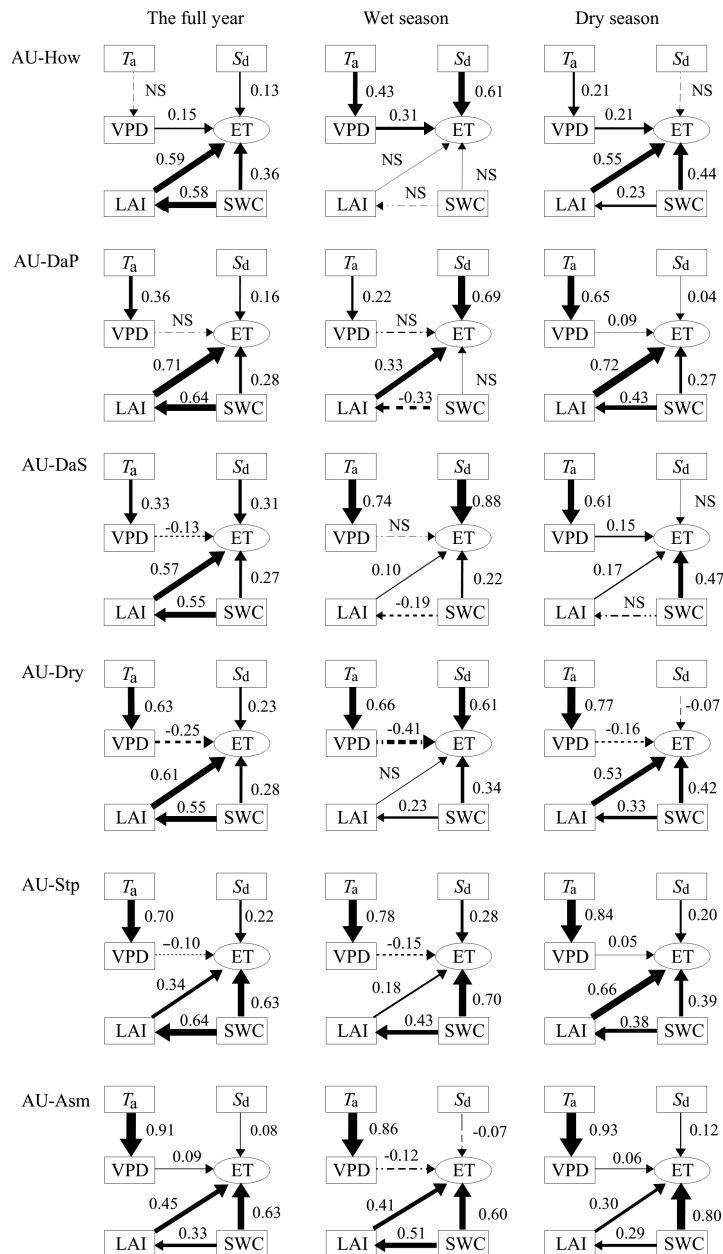


Figure 13. Path diagrams illustrating the influences of  $S_d$ ,  $T_a$ , VPD, SWC and LAI on ET during the full year, during the wet season (Jan-Mar) and during the dry season (May-Oct) across all years at the six sites. All variables used in the analyses were daily mean values of the entire time series available indicated in Table 1.

At an annual time scale, the path values for LAI at the mesic sites (AU-How, AU-DaP and AU-DaS) ranked highest among direct path values ( $> 0.5$ ), followed by SWC (0.27~0.36). Similarly at the AU-Dry site, the effects of LAI were dominant (0.61), followed by SWC (0.28). At the driest sites, AU-Stp and AU-Asm, SWC was the most dominant variable, showing large path strength coefficient value (0.63) (Figure 13). In the wet season (Jan-Mar), the path values for  $S_d$  showed the largest strength among all the direct paths to ET and this was evident at the mesic sites (AU-How, AU-DaP, AU-DaS) and AU-Dry. AU-How and AU-DaP had no significant relationship between SWC and ET in wet season, while this was not the case for the drier sites (AU-Stp and AU-Asm), where SWC ranked as the most dominant path (Figure 13). In the dry season, only AU-Asm showed a strong direct effect of SWC on ET, while for all other sites LAI displayed the strongest direct path followed by SWC.

The seasonal pattern of Figure 14 summarises the results of Figure 13 at monthly scale.  $S_d$  was the most dominated direct path for wet season ET at the mesic sites (AU-How, AU-DaP, AU-DaS). The controlling power of  $S_d$  on ET became weaker and the effects of SWC on ET were strong for the inland sites. The effect of LAI was most profound during the dry season period for the sites AU-How, AU-Dry, AU-Stp and AU-Asm. Figure 15 illustrated the relative importance of  $S_d$ , LAI and SWC on GPP at monthly scale. The strength of  $S_d$  controlling wet season GPP also showed a declining trend for the six sites downwards the precipitation. The power of LAI controlling GPP directly was stronger than that of  $S_d$  and SWC.

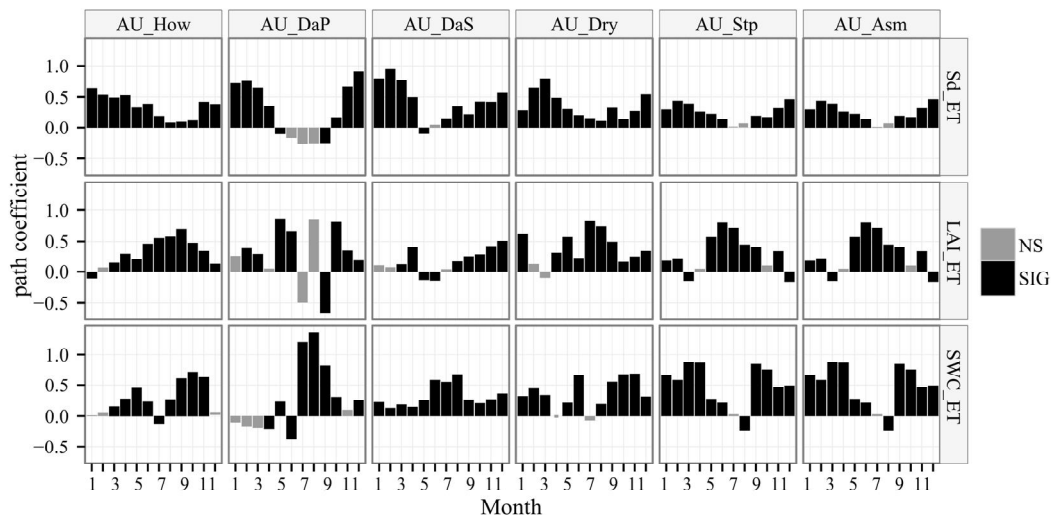


Figure 14. Path diagrams illustrating the direct effects of  $S_d$ , LAI and SWC on ET at monthly scale at the six sites. Black bar indicates significant path coefficient ( $P < 0.001$ ) and grey bar indicates nonsignificant path value.

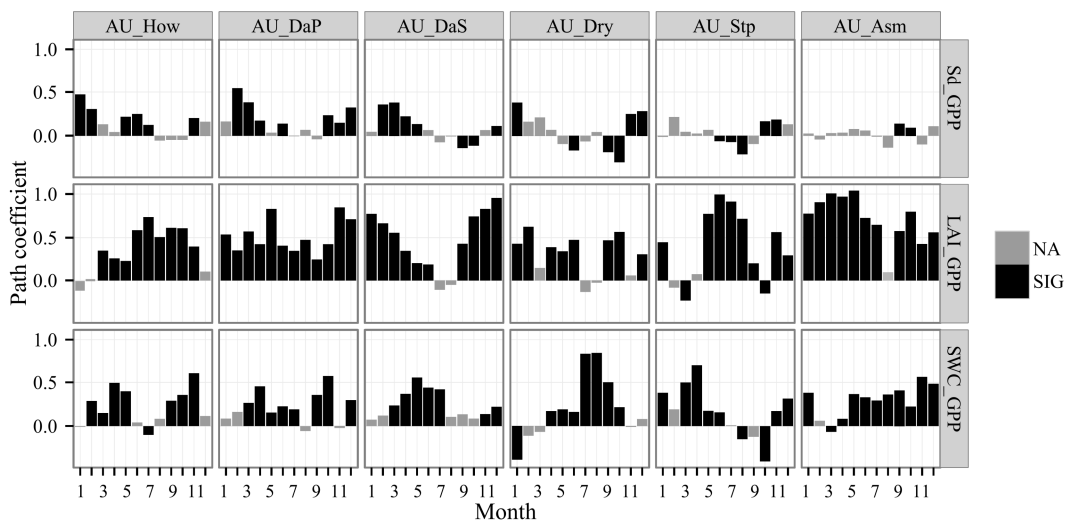


Figure 15. Path diagrams illustrating the direct effects of  $S_d$ , LAI and SWC on GPP at monthly scale at the six sites. The meaning of black bar and grey bar are the same as Figure 14.

Both regression (Figure 6) and path analysis (Figures 12 and 13) illustrated that  $S_d$  played a key role in driving wet season ET for wet and mesic savannas. At AU-How, AU-DaP and AU-DaS, wet season (Jan-Mar)  $S_d$  and ET were significantly correlated (Figure 6) and the connection strength of  $S_d$  was the highest among all variables (Figure 13). Path analysis proved to be an effective method for detecting the relative contributions of ecohydrological factors driving ET and GPP.

At wet savanna sites (e.g. AU-How), ET was not limited by SWC and soil water supply was able to meet the atmospheric demand of water (i.e. water supply equals demand) and the limitation to the equilibrium comes from available energy. The long and rainy periods in the wet season may restrict  $S_d$  and consequently ET and GPP. The limitation due to cloud cover on carbon fluxes was also illustrated by an experiment conducted in the Panama rainforest by installing high-intensity lamps over the canopy, resulting in enhanced net carbon uptake during the heavily cloud-covered rainy season (Graham et al., 2003). At the mesic site AU-How, declining surface SWC only decreased soil evaporation and did not have an effect on transpiration by trees. Enhanced tree transpiration at AU-How in the dry season was due to the increased evaporate demand and made possible by availability of deep soil-water stores was observed (O'Grady et al., 1999; Eamus et al., 2000; Hutley et al., 2000; Beringer et al., 2007). Enhanced vegetation activity in sunnier dry season was also reported in the Amazon rainforest, indicating that  $S_d$  may impose greater influence than precipitation on rainforest phenology and productivity (Huete et al., 2006).

SWC in the top 5 cm was not representative of water status of the entire soil profile and thus vegetation at AU-How can still maintain  $\alpha > 1.0$  when surface SWC was only 0.05 (Figure 8). Further southwards along the NATT, where rainfall amounts were smaller and the length of dry season increased, SWC became an increasingly important factor controlling ET and the limitation on ET switched from energy to water availability. This is especially evident at AU-Stp and AU-Asm, particularly during the wet season and at an annual scale. At these sites and during these periods, SWC became

the dominant factor controlling wet season ET. In the dry season, SWC and LAI were the two primary factors controlling ET as indicated by the path values. ET at AU-Asm strongly depended on precipitation and consequently variations of the top 10 cm soil water content, which was evident in the significant relationship between  $\alpha$  and SWC (Figure 9) and corresponding decline of  $\alpha$  with SWC during the transit of wet and dry seasons (Figure 8).  $S_d$  and SWC showed a similar pattern in the constraint of GPP and ET. The correlation of GPP to SWC was weaker than that of ET to SWC at dry sites, AU-Dry and AU-Asm (Figures 9 and 10), as a result of longer lag in response of GPP to SWC than that observed in ET (Eamus et al., 2013).

The switch from energy limitation to water limitations along precipitation gradients has also been found in other biome-type gradients (from tropical forest to savanna) in Brazil (da Rocha et al., 2009). In addition, Calder (1998) suggested that radiation and advection are the principal limitations of ET in the wet uplands of the United Kingdom, whereas plant water availability can constrain ET in semi-arid areas. The switch of energy and water limitation on ET can also occur in the same year, evident in grassland growing in Mediterranean-type climates in California, USA (Ryu et al., 2008). Half of dryland areas also experience periods of temperature or radiation constraint on vegetation growth and ET (Nemani et al., 2003; Seneviratne et al., 2010; Fensholt et al., 2012).

#### *The Contribution of LAI and the Tree:Grass Ratio to ET and GPP*

Vegetation is an important regulator for savanna function, evident in the strong link of LAI with ET and GPP in path analysis (Section 3.3). The effects of the tree:grass ratio on ET were most evident in the comparison of AU-DaP and AU-DaS, two nearby sites with different tree:grass ratios (Weinmann et al., 2009). The two sites have similar climate drivers but different seasonality in water and carbon fluxes (Figure 16). In the wet season, AU-DaP had higher LAI ( $\sim 3.0 \text{ m}^2 \text{ m}^{-2}$ ) than AU-DaS ( $\sim 1.8 \text{ m}^2 \text{ m}^{-2}$ ) and this contributed to higher ET ( $632.3 \pm 55.7 \text{ mm year}^{-1}$ ) and GPP ( $1301.5 \pm 185.0 \text{ g C year}^{-1}$ ) at AU-DaP compared with that of AU-DaU ( $585.6 \pm 38.5 \text{ mm water year}^{-1}$ ,  $1025.0 \pm 160.1 \text{ g C year}^{-1}$ ). ET and  $\alpha$  were more sensitive to surface SWC in the pasture than the savanna (Figure 9), especially during the transition between wet and dry seasons (Figure 8). In the dry season at AU-DaP, ET was mainly derived from limited amounts of soil evaporation due to the senescence of functional grasses, thus ET and GPP were low ( $122.0 \pm 44.9 \text{ mm water year}^{-1}$ ,  $141.0 \pm 77.6 \text{ g C year}^{-1}$ ). At the annual scale, AU-DaS evaporated more water ( $903.8 \text{ mm year}^{-1}$ ) than AU-DaP ( $754.3 \text{ mm year}^{-1}$ ) as a result of the utilization of deep soil water storage by trees during dry season. Longer periods of vegetation activity also contributed slightly higher GPP ( $1489.1 \text{ g C year}^{-1}$ ) at AU-DaS than AU-DaP ( $1442.5 \text{ g C year}^{-1}$ ).

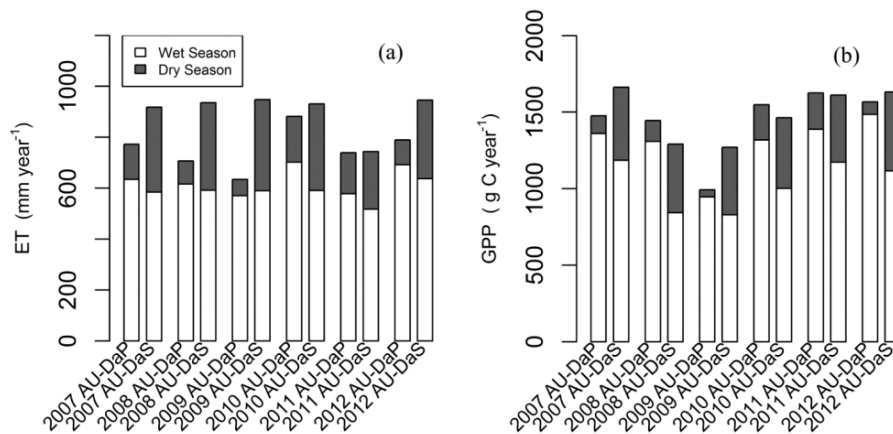


Figure 16. Seasonal amounts of ET (a) and GPP (b) at the sites AU-DaP and AU-DaS during the year 2007-2012 (blank, wet season; grey, dry season).

## Conclusions

A shift in the constraints on ET and GPP from radiation availability to moisture availability under Budyko framework was identified along the North Australian Tropical Transect. At the wet site AU-How, ET was mainly limited by  $E_{eq}$  and ultimately by available energy at the annual scale, except during the hot, dry period before the first monsoon rains. The semi-arid grassland AU-Stp and Mulga site AU-Asm sites were responded to rainfall pulses and the resultant fluctuations in SWC. We presented the impact of tree:grass ratio on ET and GPP utilizing two nearby sites covered with pasture and savanna, respectively. With a lower tree:grass ratio, AU-DaP evaporated more water and absorbed more carbon than the savanna site AU-DaS in wet season. However, the inactivity of grass during dry season resulted in annual ET and GPP at AU-DaP exceeding those at AU-DaS. Understanding the seasonality of controls on ET and GPP is of great importance for improving ET and GPP estimates. Identifying the relative importance of climate variables and tree:grass ratio on seasonal patterns of water use by vegetation will help us to identify the key factors in improvements of ET and GPP simulation. Our next work will focus on improving modelled ET estimates following the current study.

## Acknowledgements

The work was part of the project 'Australian Savanna Landscapes: Past, Present and future'. This study was funded by the Australian Research Council (DP130101566), the Australian Government's Terrestrial Ecosystems Research Network (TERN) ([www.tern.gov.au](http://www.tern.gov.au)) and the National Centre for Groundwater Research and Training (NCGRT). This work was supported also by OzFlux and the Australian Supersite Network, both parts of TERN and the latter of which is a research infrastructure facility established under the National Collaborative Research Infrastructure Strategy and Education Infrastructure Fund, Super Science Initiative, through the Department of Industry, Innovation, Science, Research and Tertiary Education.

## References

- Baldocchi, D., Falge, E., Gu, L.H., Olson, R., Hollinger, D., Running, S., Anthoni, P., Bernhofer, C., Davis, K., Evans, R., Fuentes, J., Goldstein, A., Katul, G., Law, B., Lee, X.H., Malhi, Y., Meyers, T., Munger, W., Oechel, W., U, K.T.P., Pilegaard, K., Schmid, H.P., Valentini, R., Verma, S., Vesala, T., Wilson, K., Wofsy, S., 2001. FLUXNET: A new tool to study the temporal and spatial variability of ecosystem-scale carbon dioxide, water vapor and energy flux densities. *Bull. Amer. Meteor. Soc.* 82, 2415-2434.
- Baldocchi, D., Xu, L., Kiang, N., 2004. How plant functional-type, weather, seasonal drought and soil physical properties alter water and energy fluxes of an oak-grass savanna and an annual grassland. *Agric. For. Meteorol.* 123, 13-39.
- Bassow, S.L., Bazzaz, F.A., 1998. How environmental conditions affect canopy leaf-level photosynthesis in four deciduous tree species. *Ecology.* 79, 2660-2675.
- Beringer, J., Hacker, J., Hutley, L.B., Leuning, R., Arndt, S.K., Amiri, R., Bannehr, L., Cernusak, L.A., Grover, S., Hensley, C., Hocking, D., Isaac, P., Jamali, H., Kanniah, K., Livesley, S., Neininger, B., Paw U, K.T., Sea, W., Straten, D., Tapper, N., Weinmann, R., Wood, S., Zegelin, S., 2011a. SPECIAL-Savanna Patterns of Energy and Carbon Integrated across the Landscape. *Bull. Amer. Meteor. Soc.* 92, 1467-1485.
- Beringer, J., Hutley, L.B., Hacker, J.M., Neininger, B., Paw U, K.T., 2011b. Patterns and processes of carbon, water and energy cycles across northern Australian landscapes: From point to region. *Agric. For. Meteorol.* 151, 1409-1416.
- Beringer, J., Hutley, L.B., Tapper, N.J., Cernusak, L.A., 2007. Savanna fires and their impact on net ecosystem productivity in North Australia. *Global Change Biol.* 13, 990-1004.
- Bowman, D.M.J.S., Brown, G.K., Braby, M.F., Brown, J.R., Cook, L.G., Crisp, M.D., Ford, F., Haberer, S., Hughes, J., Isagi, Y., Joseph, L., McBride, J., Nelson, G., Ladiges, P.Y., 2010. Biogeography of the Australian monsoon tropics. *J. Biogeogr.* 37, 201-216.
- Braithwaite, R.W., Estbergs, J., 1988. Tuning in to the six seasons of the wet-dry tropics. *Australian Natural History.* 22, 445-449.
- Budyko, M.I., 1958. The heat balance of the Earth's surface. National. Weather Service., U.S. Dept. of Commerce., Washington, D.C.
- Budyko, M.I., 1974. *Climate and Life.* Academic Press, New York, NY.
- Calder, I.R., 1998. Water-resource and land-use issues, SWIM Pap. 3, International Water Manage. Inst., Colombo, Sri Lanka.
- Churkina, G., Running, S.W., 1998. Contrasting Climatic Controls on the Estimated Productivity of Global Terrestrial Biomes. *Ecosystems.* 1, 206-215.
- Cleverly, J., 2011. Alice Springs Mulga OzFlux site. OzFlux: Australian and New Zealand Flux Research and Monitoring Network, hdl: 102.100.100/8697.
- Cleverly, J., Boulain, N., Villalobos-Vega, R., Grant, N., Faux, R., Wood, C., Cook, P.G., Yu, Q., Leigh, A., Eamus, D., 2013. Dynamics of component carbon fluxes in a semi-arid Acacia woodland, central Australia. *J. Geophys. Res. Biogeosciences.* 118, 1168-1185.
- Cook, G.D., Heerdegen, R.G., 2001. Spatial variation in the duration of the rainy season in monsoonal Australia. *Int. J. Climatol.* 21, 1723-1732.
- da Rocha, H.R., Manzi, A.O., Cabral, O.M., Miller, S.D., Goulden, M.L., Saleska, S.R., R-Coupe, N., Wofsy, S.C., Borma, L.S., Artaxo, P., Vourlitis, G., Nogueira, J.S., Cardoso, F.L., Nobre, A.D., Kruijt, B., Freitas, H.C., von Randow, C., Aguiar, R.G., Maia, J.F., 2009. Patterns of water and heat flux across a biome gradient from tropical forest to savanna in Brazil. *J. Geophys. Res. Biogeosciences.* 114, G00B12.
- Dewey, D.R., Lu, K.H., 1959. A correlation and path-coefficient analysis of components of crested wheatgrass seed production. *Agron. J.* 9, 515-518.
- Donohue, R.J., Roderick, M.L., McVicar, T.R., 2007. On the importance of including vegetation dynamics in Budyko's hydrological model. *Hydrol. Earth Syst. Sci.* 11, 983-995.
- Donohue, R.J., Roderick, M.L., McVicar, T.R., 2010. Can dynamic vegetation information improve the accuracy of Budyko's hydrological model? *J. Hydrol.* 390, 23-34.
- Donohue, R.J., Roderick, M.L., McVicar, T.R., 2012. Roots, storms and soil pores: Incorporating key ecohydrological processes into Budyko's hydrological model. *J. Hydrol.* 436-437, 35-50.
- Eamus, D., 2003. How does ecosystem water balance affect net primary productivity of woody ecosystems? *Funct. Plant Biol.* 30, 187-205.

- Eamus, D., Cleverly, J., Boulain, N., Grant, N., Faux, R., Villalobos-Vega, R., 2013. Carbon and water fluxes in an arid-zone *Acacia* savanna woodland: An analyses of seasonal patterns and responses to rainfall events. *Agric. For. Meteorol.* 182-183, 225-238.
- Eamus, D., O'Grady, A.P., Hutley, L., 2000. Dry season conditions determine wet season water use in the wet-tropical savannas of northern Australia. *Tree Physiol.* 20, 1219-1226.
- Fu, B.P., 1981. On the calculation of the evaporation from land surface [in Chinese], *Chin. J. Atm. Sci.* 5 (1), 23-31.
- Fensholt, R., Langanke, T., Rasmussen, K., Reenberg, A., Prince, S.D., Tucker, C., Scholes, R.J., Le, Q.B., Bondeau, A., Eastman, R., Epstein, H., Gaughan, A.E., Hellden, U., Mbow, C., Olsson, L., Paruelo, J., Schweitzer, C., Seaquist, J., Wessels, K., 2012. Greenness in semi-arid areas across the globe 1981–2007 – an Earth Observing Satellite based analysis of trends and drivers. *Remote Sens. Environ.* 121, 144-158.
- Glenn, E.P., Doody, T.M., Guerschman, J.P., Huete, A.R., King, E.A., McVicar, T.R., Van Dijk, A.I.J.M., Van Niel, T.G., Yebra, M., Zhang, Y., 2011. Actual evapotranspiration estimation by ground and remote sensing methods: the Australian experience. *Hydrol. Processes.* 25, 4103-4116.
- Grace, J.B., Bollen, K.A., 2005. Interpreting the Results from Multiple Regression and Structural Equation Models. *ESA Bulletin.* 86, 283-295.
- Graham, E.A., Mulkey, S.S., Kitajima, K., Phillips, N.G., Wright, S.J., 2003. Cloud cover limits net CO<sub>2</sub> uptake and growth of a rainforest tree during tropical rainy seasons. *Proc. Natl. Acad. Sci.* 100, 572-576.
- Haverd, V., Raupach, M.R., Briggs, P.R., Canadell, J.G., Isaac, P., Pickett-Heaps, C., Roxburgh, S.H., van Gorsel, E., Viscarra Rossel, R.A., Wang, Z., 2012. Multiple observation types reduce uncertainty in Australia's terrestrial carbon and water cycles. *Biogeosciences Discuss.* 9, 12181-12258.
- Huete, A.R., Didan, K., Shimabukuro, Y.E., Ratana, P., Saleska, S.R., Hutyra, L.R., Yang, W., Nemani, R.R., Myneni, R., 2006. Amazon rainforests green-up with sunlight in dry season. *Geophys. Res. Lett.* 33, L06405.
- Hutley, L.B., Beringer, J., Isaac, P.R., Hacker, J.M., Cernusak, L.A., 2011. A sub-continental scale living laboratory: Spatial patterns of savanna vegetation over a rainfall gradient in northern Australia. *Agric. For. Meteorol.* 151, 1417-1428.
- Hutley, L.B., Leuning, R., Beringer, J., Cleugh, H.A., 2005. The utility of the eddy covariance techniques as a tool in carbon accounting: tropical savanna as a case study. *Aust. J. Bot.* 53, 663-675.
- Hutley, L.B., O'Grady, A.P., Eamus, D., 2000. Evapotranspiration from Eucalypt open-forest savanna of Northern Australia. *Funct. Ecol.* 14, 183-194.
- Hutley, L.B., O'Grady, A.P., Eamus, D., 2001. Monsoonal influences on evapotranspiration of savanna vegetation of northern Australia. *Oecologia.* 126, 434-443.
- Huxman, T.E., Turnipseed, A.A., Sparks, J.P., Harley, P.C., Monson, R.K., 2003. Temperature as a control over ecosystem CO<sub>2</sub> fluxes in a high-elevation, subalpine forest. *Oecologia.* 134, 537-546.
- Jönsson, P., Eklundh, L., 2004. TIMESAT—a program for analyzing time-series of satellite sensor data. *Comput. Geosci.* 30, 833-845.
- Jones, J.A., Creed, I.F., Hatcher, K.L., Warren, R.J., Adams, M.B., Benson, M.H., Boose, E., Brown, W.A., Campbell, J.L., Covich, A., Clow, D.W., Dahm, C.N., Elder, K., Ford, C.R., Grimm, N.B., Henshaw, D.L., Larson, K.L., Miles, E.S., Miles, K.M., Sebestyen, S.D., Spargo, A.T., Stone, A.B., Vose, J.M., Williams, M.W., 2012. Ecosystem Processes and Human Influences Regulate Streamflow Response to Climate Change at Long-Term Ecological Research Sites. *Bioscience.* 62, 390-404.
- Jung, M., Reichstein, M., Ciais, P., Seneviratne, S.I., Sheffield, J., Goulden, M.L., Bonan, G., Cescatti, A., Chen, J.Q., de Jeu, R., Dolman, A.J., Eugster, W., Gerten, D., Gianelle, D., Gobron, N., Heinke, J., Kimball, J., Law, B.E., Montagnani, L., Mu, Q.Z., Mueller, B., Oleson, K., Papale, D., Richardson, A.D., Rouspard, O., Running, S., Tomelleri, E., Viovy, N., Weber, U., Williams, C., Wood, E., Zaehle, S., Zhang, K., 2010. Recent decline in the global land evapotranspiration trend due to limited moisture supply. *Nature.* 467, 951-954.
- Kanniah, K.D., Beringer, J., Hutley, L.B., 2010. The comparative role of key environmental factors in determining savanna productivity and carbon fluxes: A review, with special reference to northern Australia. *Prog Phys Geo.* 34, 459-490.
- Kanniah, K.D., Beringer, J., Hutley, L.B., 2011. Environmental controls on the spatial variability of savanna productivity in the Northern Territory, Australia. *Agric. For. Meteorol.* 151, 1429-1439.
- Koch, G., Vitousek, P., Steffen, W., Walker, B., 1995. Terrestrial transects for global change research. *Vegetatio.* 121, 53-65.
- Li, C., 1981. *Path analysis: a primer*, 3rd edn. Boxwood, Pacific Grove, Calif.

- Ma, X., Huete, A., Yu, Q., Coupe, N.R., Davies, K., Broich, M., Ratana, P., Beringer, J., Hutley, L.B., Cleverly, J., Boulain, N., Eamus, D., 2013. Spatial patterns and temporal dynamics in savanna vegetation phenology across the North Australian Tropical Transect. *Remote Sens. Environ.* 139, 97-115.
- McVicar, T.R., Roderick, M.L., Donohue, R.J., Li, L.T., Van Niel, T.G., Thomas, A., Grieser, J., Jhajharia, D., Himri, Y., Mahowald, N.M., Mescherskaya, A.V., Kruger, A.C., Rehman, S., Dinpashoh, Y., 2012. Global review and synthesis of trends in observed terrestrial near-surface wind speeds: Implications for evaporation. *J. Hydrol.* 416, 182-205.
- Nemani, R.R., Keeling, C.D., Hashimoto, H., Jolly, W.M., Piper, S.C., Tucker, C.J., Myneni, R.B., Running, S.W., 2003. Climate-Driven Increases in Global Terrestrial Net Primary Production from 1982 to 1999. *Science.* 300, 1560-1563.
- O'Grady, A.P., Eamus, D., Hutley, L.B., 1999. Transpiration increases during the dry season: patterns of tree water use in eucalypt open-forests of northern Australia. *Tree Physiol.* 19, 591-597.
- Olivas, P.C., Oberbauer, S.F., Tweedie, C.E., Oechel, W.C., Kuchy, A., 2010. Responses of CO<sub>2</sub> flux components of Alaskan Coastal Plain tundra to shifts in water table. *J. Geophys. Res. Biogeosciences* 115, G00I05.
- Poulter, B., Frank, D., Ciais, P., Myneni, R.B., Andela, N., Bi, J., Broquet, G., Canadell, J.G., Chevallier, F., Liu, Y.Y., Running, S.W., Sitch, S., van der Werf, G.R., 2014. Contribution of semi-arid ecosystems to interannual variability of the global carbon cycle. *Nature.* 509, 600-603.
- Priestley, C.H.B., Taylor, R.J., 1972. On the Assessment of Surface Heat Flux and Evaporation Using Large-Scale Parameters. *Mon Weather Rev.* 100, 81-92.
- Rahman, A.F., Sims, D.A., Cordova, V.D., El-Masri, B.Z., 2005. Potential of MODIS EVI and surface temperature for directly estimating per-pixel ecosystem C fluxes. *Geophys. Res. Lett.* 32, 32L19404.
- Raupach, M.R., 2001. Combination theory and equilibrium evaporation. *Q. J. R. Meteor. Soc.* 127, 1149-1181.
- Rodrigues, T.R., Vourlitis, G.L., Lobo, F.D., de Oliveira, R.G., Nogueira, J.D., 2014. Seasonal variation in energy balance and canopy conductance for a tropical savanna ecosystem of south central Mato Grosso, Brazil. *J. Geophys. Res. Biogeosciences.* 119, 1-13.
- Rosseel, Y., 2012. lavaan: An R Package for Structural Equation Modeling. *J Statist Soft.* 48, 1-36.
- Ryu, Y., Baldocchi, D.D., Ma, S., Hehn, T., 2008. Interannual variability of evapotranspiration and energy exchange over an annual grassland in California. *J. Geophys. Res. Atmospheres.* 113, D09104.
- Safriel, U., Adeel, Z., Niemeijer, D., Puigdefabregas, J., White, R., Lal, R., Winslow, M., Ziedler, J., Prince, S., Archer, E., King, C.S., Barry, Wessels, K., Nielsen, T., Portnov, B., Reshef, I., Thonell, J., Lachman, E. and McNab, D., 2005. Dryland Systems. In: Hassan, R., Scholes, R., Ash, N. (Eds.), *Ecosystems and Human Well-Being: Current State and Trends.* Island Press, Washington DC.
- Saito, M., Kato, T., Tang, Y., 2009. Temperature controls ecosystem CO<sub>2</sub> exchange of an alpine meadow on the northeastern Tibetan Plateau. *Global Change Biol.* 15, 221-228.
- Seneviratne, S.I., Corti, T., Davin, E.L., Hirschi, M., Jaeger, E.B., Lehner, I., Orlowsky, B., Teuling, A.J., 2010. Investigating soil moisture-climate interactions in a changing climate: A review. *Earth-Sci. Rev.* 99, 125-161.
- Shi, H., Li, L., Eamus, D., Cleverly, J., Huete, A., Beringer, J., Yu, Q., Gorsel, E.v., Hutley, L., 2014. Intrinsic climate dependency of ecosystem light and water-use-efficiencies across Australian biomes. *Environmental Research Letters* 9, 104002.
- Tang, Y., Wen, X., Sun, X., Zhang, X., Wang, H., 2014. The limiting effect of deep soilwater on evapotranspiration of a subtropical coniferous plantation subjected to seasonal drought. *Adv. Atmos. Sci.* 31, 385-395.
- Teuling, A.J., Hirschi, M., Ohmura, A., Wild, M., Reichstein, M., Ciais, P., Buchmann, N., Ammann, C., Montagnani, L., Richardson, A.D., Wohlfahrt, G., Seneviratne, S.I., 2009. A regional perspective on trends in continental evaporation. *Geophys. Res. Lett.* 36, L02404.
- Trenberth, K.E., Fasullo, J.T., Kiehl, J., 2009. Earth's Global Energy Budget. *Bull. Amer. Meteor. Soc.* 90, 311-323.
- Ueyama, M., Iwata, H., Harazono, Y., 2014. Autumn warming reduces the CO<sub>2</sub> sink of a black spruce forest in interior Alaska based on a nine-year eddy covariance measurement. *Global Change Biol.* 20, 1161-1173.
- Weinmann, R.A., Isaac, P.R., Hutley, L.B., Beringer, J., Grover, S., 2009. Surface energy balance from three land cover classes in a tropical savanna of the Daly River catchment, Northern Territory. *iLEAPS Science Conference, Melbourne August, 24-28.*

- Whitley, R.J., Macinnis-Ng, C.M.O., Hutley, L.B., Beringer, J., Zeppel, M., Williams, M., Taylor, D., Eamus, D., 2011. Is productivity of mesic savannas light limited or water limited? Results of a simulation study. *Global Change Biol.* 17, 3130-3149.
- Williams, R.J., Duff, G.A., Bowman, D.M.J.S., Cook, G.D., 1996. Variation in the composition and structure of tropical savannas as a function of rainfall and soil texture along a large-scale climatic gradient in the Northern Territory, Australia. *J. Biogeogr.* 23, 747-756.
- Williams, R.J., Myers, B.A., Muller, W.J., Duff, G.A., Eamus, D., 1997. Leaf phenology of woody species in a north Australian tropical savanna. *Ecology.* 78, 2542-2558.
- Xiao, X., Zhang, Q., Hollinger, D., Aber, J., Moore, B., 2005. Modeling gross primary production of an evergreen needleleaf forest using MODIS and climate data. *Ecol. Appl.* 15, 954-969.
- Zhang, L., Dawes, W.R., Walker, G.R., 2001. Response of mean annual evapotranspiration to vegetation changes at catchment scale. *Water Resour. Res.* 37, 701-708.
- Zhang, L., Hickel, K., Dawes, W.R., Chiew, F.H.S., Western, A.W., Briggs, P.R., 2004. A rational function approach for estimating mean annual evapotranspiration. *Water Resour. Res.* 40, W02502, doi: 02510.01029/02003WR00271.
- Zhu, X.J., Yu, G.R., Hu, Z.M., Wang, Q.F., He, H.L., Yan, J.-H., Wang, H.M., Zhang, J.H., 2015. Spatiotemporal variations of T/ET (the ratio of transpiration to evapotranspiration) in three forests of Eastern China. *Ecol. Indicators.* 52, 411-421.

